CONF-801011--24

MASTER

GA-A16069

THERMAL-HYDRAULICS DESIGN COMPARISONS FOR THE TANDEM MIRROR HYBRID REACTOR BLANKET

by

C. P. C. WONG, Y. S. YANG and K. R. SCHULTZ

SEPTEMBER 1980

GENERAL ATOMIC COMPANY

GA-A16069

THERMAL-HYDRAULICS DESIGN COMPARISONS FOR THE TANDEM MIRROR HYBRID REACTOR BLANKET

by

C. P. C. WONG, Y. S. YANG and K. R. SCHULTZ

This is a preprint of a paper to be presented at the Fourth ANS Topical Meeting on the Technology of Controlled Nuclear Fusion, October 14-17, 1980, King of Prussia, Pennsylvania.

Work supported by
Department of Energy
Contract DE-AT03-76ET51011

GENERAL ATOMIC PROJECT 3235
SEPTEMBER 1980

GENERAL ATOMIC COMPANY

THERMAL-HYDRAULICS DESIGN COMPARISONS FOR THE TANDEM MIRROR HYBRID REACTOR BLANKET*

C.P.C. Wong, Y.S. Yang† and K.R. Schultz
General Atomic Company
P.O. Box 81608
San Diego, California 92138

The Tandem Mirror Hybrid Reactor (TMHR) is a cylindrical reactor, and the fertile materials and tritium breeding fuel elements can be arranged with radial or axial orientation in the blanket module. Thermal-hydraulics performance comparisons were made between plate, axial rod and radial rod fuel geometries. The three configurations result in different coolant/void fractions and different clad/ structure fractions. The higher void fraction in the two rod designs means that these blankets will have to be thicker than the plate design blanket in order to achieve the same level of nuclear interactions. Their higher structural fractions will degrade the uranium breeding ratio and energy multiplication factor of the design. One difficulty in the thermal-hydraulics analysis of the plate design was caused by the varying energy multiplication of the blanket during the lifetime of the plate which forced the use of designs that operated in the transition flow regime at some point during life. To account for this, an approach was adopted from Gas Cooled Fast Reactor (GCFR) experience for the pressure drop calculation and the corresponding heat transfer coefficient that was used for the film drop thermal calculation. Because of the superior nuclear performance, the acceptable thermal-hydraulic characteristics and the mechanical design feasibility, the plate geometry concept was chosen for the reference gas-cooled TMHR blanket design.

Introduction

The Tandem Mirror Hybrid Reactor (TMHR) Study[1] was sponsored by DOE and jointly carried out by Lawrence Livermore Laboratory, General Atomic Company, General Electric Company and Bechtel Corporation in developing concepts for commercial fusion-fission hybrid reactors. General Atomic Company designed a helium-cooled TMHR blanket using Th-metal as the fertile material, with an average thermal power of 4000 MW and a production of 2.7 metric tons of ^{233}U per year. This design which is within the imposed temperature and pressure drop limits was developed with careful integration of the mechanical, neutronics and thermal-hydraulics design considerations.

The approaches adapted in this thermal-hydraulics design are generic in nature and should be applicable to other blanket designs. The comparison of blanket configuration is crucial in minimizing blanket thickness and maximizing neutronics performances and should be performed as a part of the initial thermal-hydraulics design of fusion blanket elements.

*Work supported by Department of Energy, Contract DE-AT03-76ET51011.
†Present address: Department of Mechanical Engineering, University of Texas, Austin, Texas.

The thermal hydraulic design of a gas-cooled reactor system should have high thermal efficiency and low pressure losses. The high efficiency requirement dictates a high coolant outlet temperature, restricted by the maximum operating temperature limits of the reactor materials. The low pressure loss requirement leads to high system operating pressure to obtain high coolant density, a large coolant inlet-to-outlet temperature differential, and restricts the velocities of the coolant in various sections of the coolant loop. On the other hand, the restrictions on material operating temperature limits lead to high coolant velocities to maintain high heat transfer coefficients.

Thermal-hydraulics analysis of the TMHR was performed to establish the temperature and pressure drop characteristics of the first-wall and the breeder sections. The approaches to the problems and the key equations used in these calculations are presented in this paper.

The energy balance equation was used to calculate the coolant temperature at positions of interest from the local volumetric heat generation rates. Knowing the dimensions of the fuel element, the heat flux was calculated. The convective and conductive heat transfer equations were then used to calculate cladding and material temperatures. Hot-spot factors were included to account for manufacturing defects and material inhomogeneity. In calculating the pressure drops, the energy balance equation was used to calculate the coolant velocity, by knowing the power generated, the geometry of the flow channel and the inlet-outlet coolant temperature differential. Knowing the fluid velocity, the friction factor was calculated, which was then used to calculate the pressure drops. Care was taken to distinguish between the laminar regime with Re <3000 and the turbulent regime with Re >6000 and to avoid operating in the transitional unstable regime whenever possible. Yet due to the difference in blanket energy multiplication at the beginning and at the end of life, the coolant in the plate design would have to be operating in the transition regime, and an approach was adopted to calculate the heat-transfer coefficient in this regime.

Three Fuel Element Configurations of Blanket Design

In order to select the best fuel element configuration of blanket design for the TMHR study, three configurations were considered as shown in Fig 1. They are the simple plate design; the axial rod, radial flow design; and the radial rod, radial flow design. The descriptions of these designs are presented in this section.

Figure 1(a) shows a schematic of the tapered fuel plates. Each plate has three sections, a 12 cm Th-metal section, a 45 cm Li_2O section and a 10 cm section of stainless-steel hot shield. The plate is tapered from a thickness of 1.15 cm at the narrow end to 1.58 cm at the wider end. Helium coolant leaving the first wall area flows in from the narrow edge toward the thicker edge through the wire-wrap gaps between the plates. The plates, each 50 cm long, are supported from the ends by a grid structure which also contains the piping for the thorium plate pressure equalization system and the Li_2O plate tritium purge system. The plate assemblies are stacked together to cover the length of the reactor. This coverage of the reactor central area would capture more than 95% of the fusion neutron energy. The slits at the narrow ends of the plates are to accommodate the change in plate dimensions and relieve the strain due to neutron induced swelling.[2]

The primary functions of the clad are to separate the plates, to support the thorium and Li_2O fuel materials, to contain the Li_2O and to confine the T_2O that is produced from the tritium breeding reaction. Because the vented clad does not have to carry much load, mainly the weight of thorium and Li_2O, a higher temperature limit of 665°C was used for Inconel 718, whereas the temperature limit of the first wall is 550°C. The centerline temperature

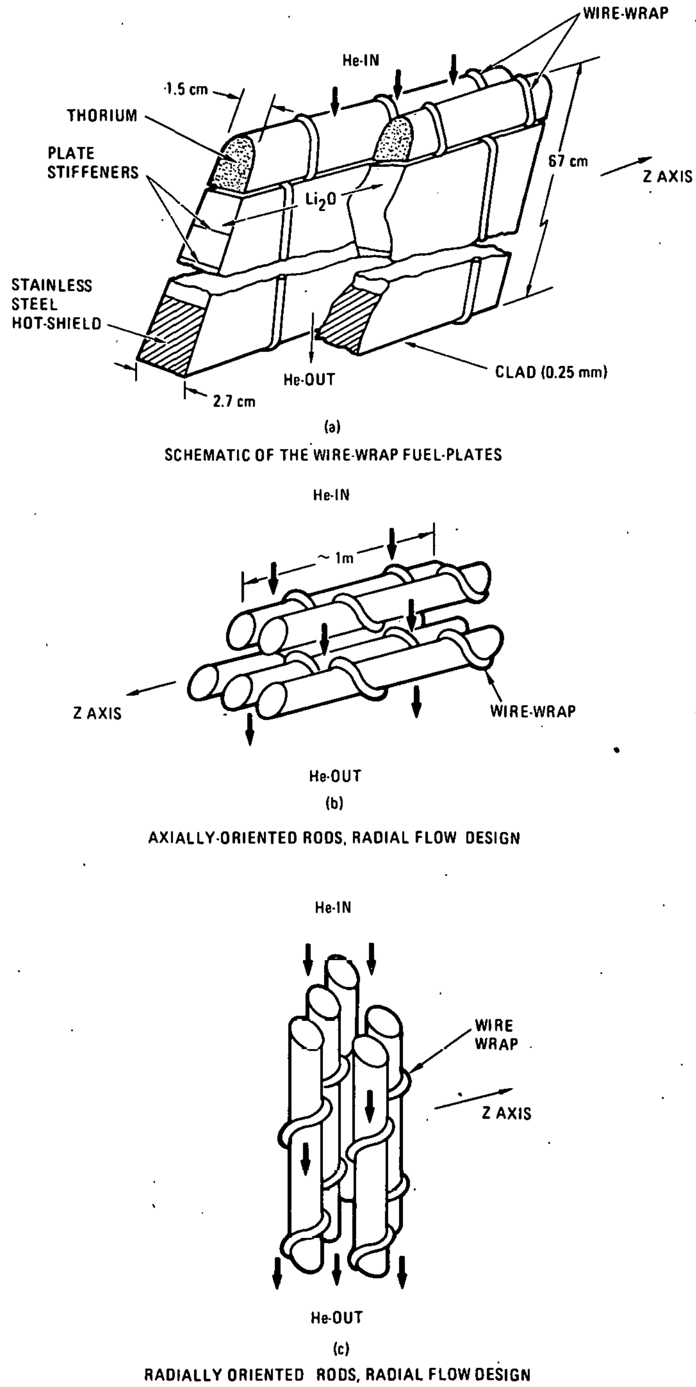

Fig. 1. Fuel element configurations.

limit of the plate was taken as the melting point of Li_2O at about 1700°C. The clad thickness was taken to be as thin as reasonable from a manufacturing standpoint, about 1/4 mm. The He gap width was fixed at 1 mm to keep the convective heat transfer coefficient high, without exceeding the fuel zone coolant pressure drop limit of 20.7 kPa (3 psi). The coolant gaps are small and tight tolerances are needed for the wire-wrap plate design in order to minimize hot spots from flow non-uniformities.

Design calculations were made for axially-oriented rods with radial flow in the blanket of TMHR as shown in Fig. 1(b). The rods can be fairly long (∿1 m) by putting them in the axial direction in the blanket module, which may reduce the blanket cost. Further, the rods would be easier to manufacture than plates. A preliminary analysis was done to determine the optimized design within the allowable thermal and mechanical constraints.

In order to compare the plate design with the axial rod design, the coolant inlet-outlet differential was set at 230°C and the coolant pressure drop was set at 20.7 kPa (3 psi). An analysis based on the coolant operating conditions at the blanket end of life was made. Because of the exponentially decreasing distribution of the nuclear volumetric heating from the first wall outward, the heat source for the axial rod calculation is that from the rod next to the first wall which would given an indication of the worst situation. The inlet temperature of helium to the fuel region is 300°C and the volumetric heat generation rate is 120 MW/m^3 at the end of life of 9.6 $MW\text{-}yr/m^2$. The axial rod was designed with annular fuel pellets to allow swelling from neutron irradiation. By a conservative evaluation, maximum volumetric swelling of thorium metal is about 2%, which corresponds to a linear expansion of 0.7%.

The third fuel configuration considered is that of radially oriented rods with radial coolant flow, as shown in Figure 1(c). Use of this configuration for gas-cooled hybrid blankets under the same flow conditions and with the same fuel geometry has been studied by S. Rao and C. Baxi with U_3Si as fertile material for the Standard Mirror Hybrid Reactor design.[3] The basic strategy and calculation method are the same as in the previous studies.

The fuel rod in the blanket is made of three different zones. Thorium is placed in the first zone as fertile material, followed by Li_2O in the center part of the rod as the tritium breeding zone. The end part of the blanket is composed of a 10 cm stainless steel 316 reflector/shield. Since the limiting rod diameter occurs in the thorium zone, future studies should investigate use of larger rods in the lithium and reflector/shield zones.

Input from Neutronics Results

Since more than 99% of the total thermal energy from nuclear interactions is deposited in the blanket section and the first wall, it is crucial to know the spatial distribution of the energy deposition and to design the blanket thermal-hydraulics accordingly. Figure 2 gives

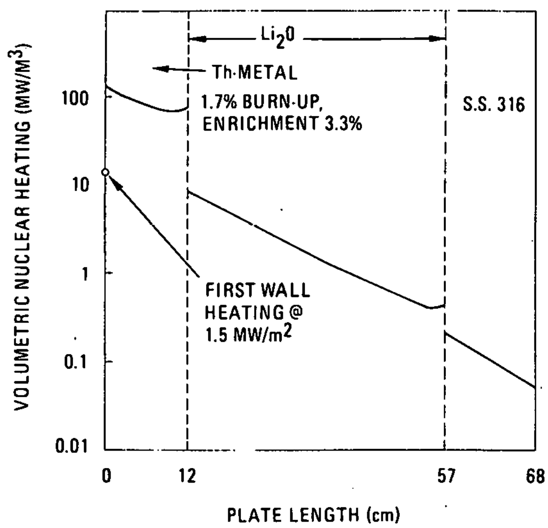

Fig. 2. Blanket end-of-life power density for the plate design (at 9.6 $MW\text{-}yr/m^2$).

the volumetric nuclear heating (MW/m^3) in the plate design blanket as a function of distance from the first wall. The energy deposition decreases roughly exponentially from the first wall. For this reason the designs are such that the coolant is first routed to the first wall and then passes radially outward through the fuel element section, putting the lowest helium temperature in the region of highest power density. This figure shows the energy output at the highest energy multiplication, which is found at the end of life.

Thermal-Hydraulics Analysis

This section presents the thermal-hydraulics equations that are applicable for the three fuel element configurations which are under consideration.

Plate Design

The equations used were those applicable to flat plates which can adequately represent the geometry of flat-plate type first wall and breeder plates.

The following key equations were used in calculating the temperature distributions:

$$h = 8.23\ k/D_e \qquad \text{for Re} < 3000$$

$$h = 0.021\ Re^{0.8}Pr^{0.6}k\varepsilon/D_e \ \text{for Re} > 6000 \quad (1)$$

where Re and Pr are the Reynolds and Prandtl numbers, k and ε are coolant thermal conductivity and roughness factor, and D_e is the equivalent diameter, coolant thermal conductivity is given by,

$$k = \mu C_p/Pr, \tag{2}$$

where μ and C_p are the coolant viscosity and specific heat,

coolant viscosity can be calculated by,

$$\mu = 3.953 \times 10^{-7} (T_c)^{0.687} \quad , \tag{3}$$

where T_c is the coolant temperature in degrees K,

coolant density,

$$\rho = P/(RT_c) \quad , \tag{4}$$

where P is the helium pressure and R is the gas constant (2077 J/kg°K),

hot spot cladding (WHSF) and fuel (CHSF) temperatures are given by,

$$T_{WHSF} = T_o + F_b\Delta T_b + F_{cf}\Delta T_f + F_c\Delta T_c \tag{5}$$

$$T_{CHSF} = T_o + F_b\Delta T_b + F_{cf}\Delta T_f + 2F_c\Delta T_c + F_g\Delta T_g + F_F\Delta T_F \quad . \tag{6}$$

The respective symbols and values used in the calculations are listed in Table 1.

The various temperature differentials were calculated by one-dimensional heat transfer conduction and convection equations. These coefficients were also used for the other two fuel element configurations.

One majority difficulty in analyzing the thermal hydraulics of the plate design was caused by the varying energy multiplication of the blanket during the lifetime (6.4 full power years) of the plate from 2.8 to 8.5 as shown in Fig. 3. In order to maintain a constant coolant outlet temperature, the coolant mass flow rate has to be changed, thus the Reynolds number would vary for a fixed plate geometry during the submodule lifetime as shown on Fig. 4. The Reynolds numbers indicate that the coolant would be operating in the transition regime at some time during blanket life even with a range of coolant inlet to outlet different, from 150 to 300°C. An appropriate method has to be developed for the calculation of heat transfer coefficients operating in this regime.

From the experience of GCFR, the heat transfer coefficient for transitional flow was obtained by first comparing the friction factors for laminar and turbulent flow at the given Reynolds number, then the higher friction

TABLE 1
HOT SPOT FACTOR VARIABLES, COEFFICIENTS AND THEIR VALUES

	Symbol (Units)	Values
Inlet temperature	T_o (C)	285
Bulk coolant temperature	ΔT_b	--
Film temperature rise	ΔT_f	--
Cladding temperature rise through half the cladding thickness	ΔT_c	--
Fuel-cladding gap temperature rise	ΔT_g	--
Fuel temperature rise	ΔT_F	--
Bulk coolant hot spot factor	F_b	1.3
Film hot spot factor for coolant	F_{cf}	1.25
Cladding hot spot factor	F_c	1.25
Fuel-cladding gap hot spot factor	F_g	1.5
Fuel hot spot factor	F_F	1.2

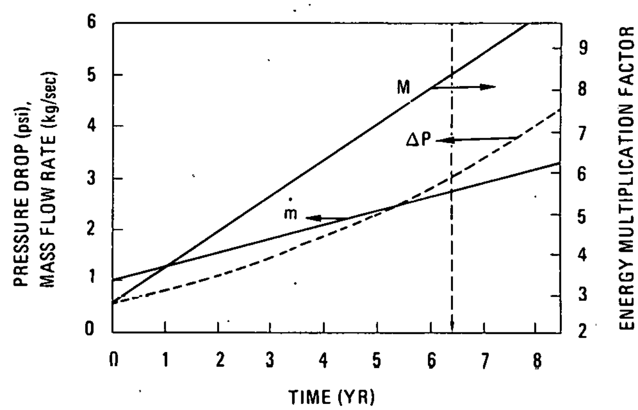

Fig. 3. Blanket energy multiplication factor (M), pressure drop (ΔP), mass flow rate (ṁ) versus time, for the plate design.

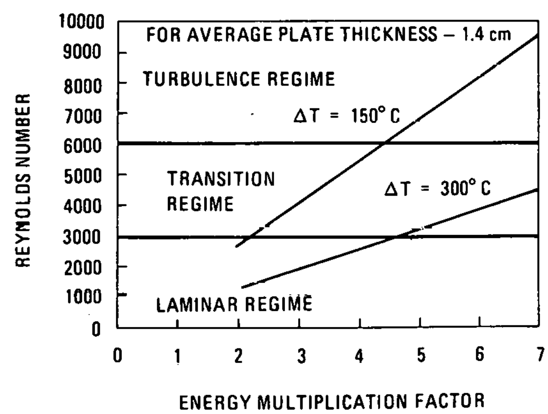

Fig. 4. Reynolds number versus blanket energy multiplication factor for coolant temperature inlet to outlet differentials of 150 and 300°C (for average plate thickness of 1.4 cm).

factor, f, was selected for the pressure drop calculation and the corresponding heat transfer coefficient was used for the film drop calculation. Calculations for the beginning and the end of life of the blanket were calculated to bracket the thermal hydraulics performance. The key equations used in the calculation of pressure drop are the following: In the laminar regime, Re <3000, the friction factor f is equal to

$$f = 16/Re \quad , \tag{7}$$

and in the turbulent regime, Re >6000

$$f = 0.0791\ Re^{-0.25} \quad . \tag{8}$$

The pressure drop is given by

$$\Delta P = 4 \frac{L}{D_e} f \frac{1}{2} \rho V^2 \quad , \tag{9}$$

where L and V are the coolant path length and average velocity, respectively.

Axially-Oriented Rods with Radial Flow Design

The temperature differentials for cylindrical rods can be calculated by the following expressions:

$$\Delta T_f = \frac{1}{h_f} \dot{q}''' \frac{(r_p^2 - r_h^2)}{2r_r} \tag{10}$$

$$\Delta T_c = \frac{t}{k_c} \dot{q}''' \frac{(r_p^2 - r_h^2)}{4(r_r - t)} \tag{11}$$

$$\Delta T_g = \frac{1}{h_g} \dot{q}''' \frac{(r_p^2 - r_h^2)}{2\iota_p} \tag{12}$$

$$\Delta T_F = \dot{q}''' \frac{r_p^2}{4k_f} \left[1 - \left(\frac{r_h}{r_p}\right)^2 - \left(\frac{r_h}{r_p}\right)^2 \ell n \left(\frac{r_p}{r_h}\right) \right] \tag{13}$$

where t = cladding thickness
r_p = radius of fuel pellet
r_h = radius of central fuel hole
r_r = radius of fuel rod (including clad)
$\dot{q}'''$ = volumetric power generation (MW/m^3)

The hot-spot temperatures were calculated by using Eqs. (9) through (13) with coefficients defined in Table 1. These equations are applicable to both the axial rod and radial rod designs.

The axially oriented rods in the blanket submodule were designed in a staggered arrangement in order to reduce neutron streaming and to enhance heat transfer. Correlations for heat transfer coefficient, friction factor and pressure drop in staggered tube banks in the turbulent-flow regime for $G_{max} D_o/\mu_f$ >6000, are as follows[4]:

$$h = \frac{k_f}{D_o} \times 0.33 \cdot \left(\frac{G_{max} D_o}{\mu_f}\right)^{0.6} \cdot Pr^{0.3} \tag{14}$$

where G_{max} = mass velocity at the minimum area,
μ_f = viscosity at film temperature,
D_o = outside rod diameter

The friction factor f can be calculated by

$$f = \left(0.25 + \frac{0.1175}{(P/D-1)^{1.08}}\right)\left(\frac{G_{max} D_o}{\mu_b}\right)^{-0.16} \quad , \tag{15}$$

for Re >6000

where P/D = pitch to diameter ratio
μ_b = viscosity at bulk temperature.

The Reynolds number in this staggered rod bank design is usually very high, thus the coolant is operated in the turbulent regime. The frictional pressure drop for flow over a bank of rods can be calculated by

$$\Delta p = \frac{2f\ G_{max}^2\ N}{\rho} \left(\frac{\mu_s}{\mu_b}\right)^{0.14} \tag{16}$$

where N = number of transverse rows of rods
μ_s = viscosity at rod surface temperature.

Radially Oriented Rods, Radial Flow Design

The thermal-hydraulic correlations for the wire-wrapped radial blanket assemblies are obtained from experimental data done by the GCFR group for a pitch-to-diameter ratio of 1.05.

The friction factor correlations are listed below:

$f = 25.72\ Re^{-0.835}$ in laminar region

$f = 0.436\ Re^{-0.263}$ in turbulent regime

The heat transfer coefficient can be calculated from the Nusselt number which is given by:

$Nu = 2.82$ in laminar flow

$Nu = 0.0203\ Re^{0.79}$ in turbulent flow

Entrance effects have also been considered in the calculation. Again, for consistency of comparison between the three fuel configurations, the inlet and outlet temperature difference is set at 230°C.

Plate Design Thermal Hydraulics Results

Figure 3 shows the variations of coolant mass flow-rate ($\dot{m}$), pressure drop (Δp) and blanket energy multiplication (M) during reactor life for the plate design. It shows that the coolant pressure drop is within the criterion of 20.7 kPa (3 psi)[1].

Figure 5 shows the temperature distributions of the plate and coolant at the beginning and the end of life (BOL and EOL). The EOL is at 9.6 MW-yr/m^2. The thermal conductivity used in the Li_2O zone was calculated as that of a mixture of Li_2O powder and static helium and would be a conservative estimate. This figure shows the satisfaction of design criteria for centerline temperature including hot spot factors of <1000°C and cladding temperature including hot spot factor of <700°C.

Table 2 summarizes the plate design parameters of the Tandem Mirror Hybrid Reactor. These parameters are the results of simple one-dimensional model calculations, principally showing the feasibility of the proposed design. Further detailed calculations and analyses will be needed during the advanced phases of the design.

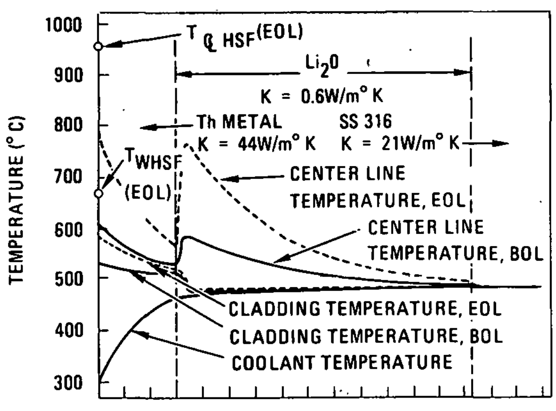

Fig. 5. Nominal temperature distributions in the blanket (K-thermal conductivity, T_{WHSF} and T_{CHSF}, wall and center-line temperature including hot spot factor).

TABLE 2
BREEDER PLATE DESIGN PARAMETERS

Fertile material	Thorium
Tritium breeding material	Li_2O
Thermal power output	4000 MW
Maximum volumetric nuclear heating	120 MW/m^3
Maximum wall loading	1.5 MW/m^2
Number of plates/submodule	24
Dimensions	
Width of plate (narrow side)	1.15 cm
Width of plate (wide side)	1.58 cm
Length of plate	50 cm
Height of plate	67 cm
Cladding thickness	0.25 mm
Width of coolant gap	1 mm
Helium parameters	
Pressure	5.6 MPa (55 atm)
Inlet temperature to fuel zone	300°C
Outlet temperature	515°C
Reynolds number	2162 → 6562
Pressure drop	2.4 → 20.7 kPa (0.35 → 3.0 psi)
Mass flow rate/module (3.5 m long)	140 → 385 kg/sec
Thermal cycle efficiency	~38%

Axial Rod, Radial Flow Design Thermal-Hydraulic Results

For this design the clad temperature is a function of both rod size and pitch to diameter ratio. The larger the rod size, the higher the clad temperature. The clad temperature is also an increasing function of pitch-to-diameter ratio. Fig. 6 shows the relation between clad temperature, rod size, and pitch to diameter ratio. Acceptable ranges for rod diameters and P/D are also indicated for clad temperature less than 665°C.

The frictional pressure drop is also a function of rod size and pitch to diameter ratio as shown in Fig. 7. For close packed arrangements (P/D <1.15), the pressure drop exceeds the design limit of 20.7 kPa (3 psi). Figure 7 also indicates the acceptable operating regime when the temperature limit is also taken into consideration. The analysis so far is based on the average heat transfer coefficient. However, with cross flow rods there would be a circumferential variation in the heat transfer coefficient around the individual rod. A conservative approximation for the

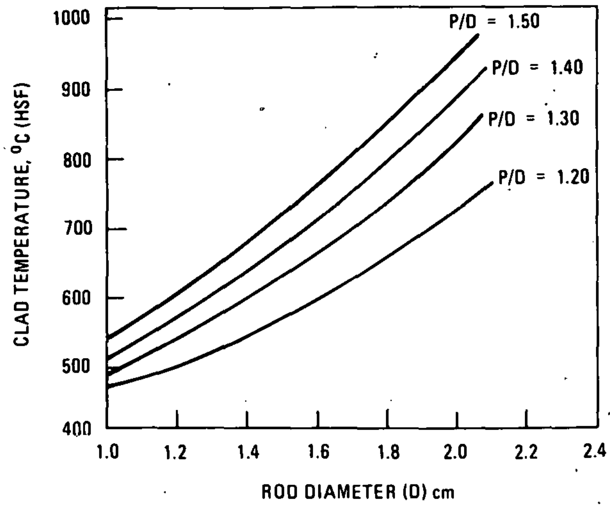

Fig. 6. Hot spot cladding temperature versus rod diameter for cross flow rods

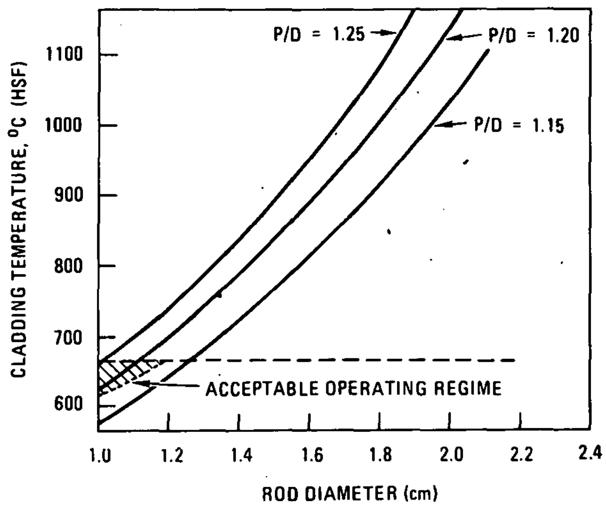

Fig. 8. Peak cladding hot spot temperature versus rod diameter for cross flow rods

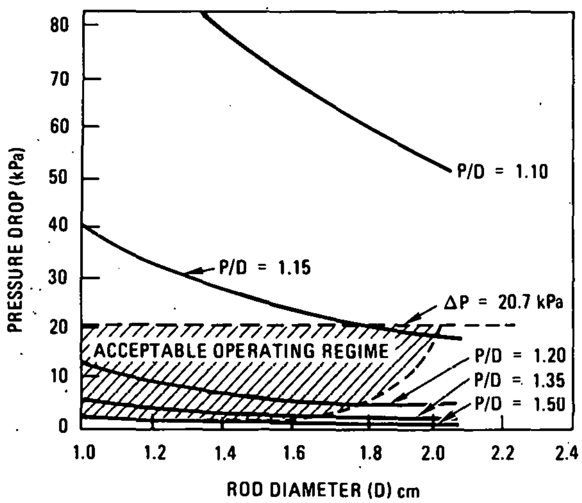

Fig. 7. Pressure drop versus rod diameter for cross flow rods

minimum local heat transfer coefficient may be obtained by considering an isolated rod. Reference 6 indicates that the minimum value of h is half of the value of the average heat transfer coefficient. As a result, the acceptable operation regime has been reduced as shown in Fig. 8.

Radial Rod, Radial Flow Design Thermal-Hydraulic Results

Because of the relatively large flow area between even close-packed rods the pressure drop is not a limiting consideration with radially oriented rods. The hot spot cladding temperature limit of 665°C limits the fuel rod diameter to 1.67 cm. The characteristics of this design are shown on Table 3.

Thermal Hydraulic Comparison

The comparison between plate, axial rod and radial rod results is tabulated in Table 3. Due to the entrance effect the maximum cladding temperature in the radial rod and plate design occurs at a few centimeters away from the front face of the fuel zone, where the volumetric heat source strength is lower than that in axial rod which has the maximum cladding temperature at the first rod in the module. This results to a higher maximum center line temperature in the axial rod case, even though it has a smaller rod diameter than the radial rod design.

Table 3 compares the thermal-hydraulic characteristics of the three fuel configuration options under equal design conditions. All three configurations result in different coolant void and clad/structure fractions. The higher void fraction in the two rod designs means that these blankets will have to be thicker than the plate design blanket in order to achieve the same level of nuclear interactions. Further, the higher structural content of the rod design blankets will degrade the nuclear performance of these concepts when compared to the plate design. The additional structural fractions shown on Table 3 will degrade the uranium breeding ratio and energy multiplication factor of the axial rod design by about 7% and the radial rod design by about 4% compared to the performance expected from the plate design blanket.

TABLE 3
FUEL CONFIGURATION THERMAL-HYDRAULIC CHARACTERISTICS

	Tapered-Plate	Axial Rod, Radial-Flow	Radial Rod, Radial Flow
Characteristic	Plate Thickness: 1.15-1.58 cm	Outer Diameter: 1.19 cm	1.67 cm
Dimension	Coolant Channel: 1 mm	Pitch/Diameter: 1.18	1.05
$\Delta T = T_{out} - T_{in}$	230°C	230°C	230°C
ΔP (kPa)	20.7	20.7	7.2
$\bar{h}$ ($W/m^2 °K$)	2434	2174	1122
$T_{max,CLAD}$	666°C	663°C	662
$T_{max,CENTERLINE}$	939°C	775°C	765°C
Reynolds Number	6562*	18212	4170
Void Fraction	7.3%	35%	17.8%
Clad/Solid Fraction	3.6%	8.2%	5.9%
Relative Breeding Performance	1	0.93	0.96

*At blanket end of life.

Conclusion

Because of the superior nuclear performance, the acceptable thermal hydraulic characteristics and the mechanical design feasibility, the plate geometry concept has been chosen for the reference gas-cooled TMHR blanket design. More detailed design and analysis of the blanket is required to fully assess the performance and feasibility concerns of the blanket. On the basis of the preliminary analysis presented here, however, the plate design is quite feasible.

References

1. R. W. Moir, et al., "Tandem Mirror Hybrid Reactor Design Study Annual Report," Lawrence Livermore Laboratory, Report UCRL-52875, to be published, 1980.
2. R. L. Creedon, "Structural Design Tolerance of Radiation Swelling - a First Step," 4th ANS Topical Meeting on the Technology of Controlled Nuclear Fusion, King of Prussia, Pennsylvania, October 14-17, 1980.
3. D. J. Bender, et al., "Reference Design for the Standard Mirror Hybrid Reactor," joint Lawrence Livermore Laboratory/General Atomic Report URCL-52478/GA-A14796, May 1978.
4. McAdams, Heat Transmission, Third Edition, McGraw-Hill, New York, 1954.
5. F. Bennet, and C. Baxi, private communication.
6. W. M. Kays, Convection Heat and Mass Transfer, McGraw-Hill, New York, 1966.

INTERNAL DISTRIBUTION

R. Bourque
S. Burnett
E. Cheng
V. Cravens
L. Creedon
D. Graumann
G. Hopkins
I. Maya
T. Ohkawa
J. Purcell
K. Schultz
C. Wong

EXTERNAL DISTRIBUTION

N. Amherd
Electric Power Research Institute
P.O. Box 10412
Palo Alto, California 94304

C. Ashworth
Pacific Gas & Electric
77 Beale St., Room 2517
San Francisco, California 94106

C. Baker
Argonne National Laboratory
9700 South Cass Avenue
Argonne, Illinois 60439

Dr. Rudi Brogli
Swiss Federal Institute for Reactor Research, E.I.R.
CH - 5305 Wurenlingen
Swizerland

G. Carlson
Lawrence Livermore National Laboratory
P.O. Box 808
Livermore, California 94550

R. Conn
University of California, Los Angeles
School of Engineering & Applied Science
Los Angeles, California 90024

J.D. Lee
Lawrence Livermore National Laboratory
P.O. Box 808
Livermore, California 94550

R.W. Moir
Lawrence Livermore National Laboratory
P.O. Box 808
Livermore, California 94550

Dr. A. Hilary Morton
Plasma Research Laboratory
Australian National University
Canberra ACT 2600, Australia

W. Neef
Lawrence Livermore Laboratory
P.O. Box 808
Livermore, California 94550

Ray Ng
Office of Fusion Energy
U.S. Department of Energy, MSG 234
Washington, D.C. 20545

D. Paul
Electric Power Research Institute
Palo Alto, California 94304

J.R. Powell
Brookhaven National Laboratory
Department of Applied Science
Upton, L.I., New York 11973

R. Scott
Electric Power Research Institute
P.O. Box 10412
Palo Alto, California 94304

G.E. Shatalov
State Committee for Utilization of Atomic Energy
Kurchatov Institute of Atomic Energy
Moscow D-182, U.S.S.R.

D.K. Sze
University of Wisconsin
Department of Nuclear Engineering
Madison, Wisconsin 53706

Dr. E.S. Weibel
Ecole Polytechnique Federal de Lausanne
CH-1007 Lausanne
21 Av. des Baines, Switzerland

Y.S. Yang
Department of Mechanical Engineering
University of Texas
Austin, Texas 78712

Dr. Li Zhengwn, or
Dr. Sun Xiang
Southwestern Institute of Physics
PO Box 15
Leshan, Sichuan
People's Republic of China